Introduction to biometrics - Iris Recognition

Fieke Hillerström (s1003828)
Bart Koornwinder (s0212083)
Laurie Overbeek (s1017926)
Sandra van der Velden (s0199273)

December 4, 2013

Abstract

In this report an iris detection system will be designed, programmed and tested. It starts off by discussing the current state of biometric systems and how they are graded. It then goes on to introduce the various steps which are taken in iris detection and which variations are possible within these steps. Out of these variations a combined method is designed, consisting of preprocessing, feature extraction and matching of the iris. In preprocessing both the iris and pupil center are detected and used to normalise the iris. The iris is then normalised using a Doubly Pair Method. The feature extraction is then performed using a Gabor filter. In matching the iris a Hamming distance is used.

In this paper three variations of this system will be tested, varying the detection method and the normalising method. A two point and a three point method of detecting the iris will be tested, and it will be tested whether or not the results improve when the outer 50% of the iris is excluded. Both for training as well as testing these systems the CASIA iris database 1.0 was used, consisting of 756 images of 108 eyes. In training, the first 70 images of ten eyes were used. The remaining images were used in the final test.

The best results were achieved by combining the two-point method and excluding the outer 50% of the iris. On the personal computer used, the system takes 3 hours to analyse the CASIA iris database. It resulted in an Equal Error Rate of 7.63% and an failure to enroll of 6.1%. Finally, recommendations will be made to further improvement of the system.

Contents

1 Introduction

Authentication of an individual's identity has become of paramount importance in our interconnected society. Biometrics is defined as the science of establishing the identity of an individual based on the inherent physical or behavioural traits associated with the person [1, 2]. Traditionally, knowledge-based schemes such as passwords and token-based schemes, such as ID-cards are used to establish identity [2]. However, these ways of authentication have several limitations. Passwords can be easily shared, ID-card can be lost or stolen, all leading to a breach in security. It is thus necessary to develop alternative methods to authenticate identity that are much harder to spoof. A way to do this, is by having a system that is based on who you are (biometrics), rather than on what you know or what you have.

1.1 Biometric system

A biometric system operates by capturing a biometric sample from a person, preprocess the extracted data and compare this recorded trait with the biometric samples in a database to determine the identity of a person (*identification*) or to verify if the person is who he claims to be (*verification*). The system can be considered to contain four parts: a sensor to capture the biometric trait, a feature extraction module to extract relevant data from the sample, a pattern classification module to provide a measure between the sample and a sample from the database and a decision module to decide whether the level of similarity is sufficient or not [2, 3]. Each of these modules will be shortly discussed.

To acquire the biometric data, a suitable biometric reader or scanner is needed. The sensor module defines the human machine interface and is therefore of great importance regarding the user acceptability. Furthermore, a high failure-to-capture rate can be the result of a poorly designed sensor [2].

The function of the feature extraction module is to extract a set of salient discriminatory features representing the underlying sample. How much information should be extracted depends on the uniqueness of the data and the capability of the classifications process [3]. Using too much information will only complicate the pattern classification, while too less information limits the ability to classify for large sample populations. During enrolment, this feature set is stored in the database and is referred to as the template [2].

To generate similarity scores, the extracted features are compared against the previously stored templates in the database. The pattern classification module calculates the similarity score. Depending on what kind of biometrics is used, the similarity score is determined in different ways. For example, in fingerprint recognition, the number of matching minutiae between the input and template feature sets is determined and reported as a match score [2].

The last module in the biometric system is the decision module. The decision module decides whether the reported similarity score is high enough to validate a claimed identity. The threshold for acceptance is a trade-off between security and usability [3].

1.2 Performance measurements

In password based systems, a perfect match is necessary to validate a users identity. However, a biometric sample is almost never exactly the same, due to imperfect sensing conditions, alterations in the users biometric characteristic and changes in ambient conditions. The distance between two feature sets originating from the same biometric trait of a user is therefore typically non-zero.

Similarity match scores can be divided in genuine and imposters scores. Genuine scores are scores resulting from matching two samples of the same user. Imposter scores result from comparing two biometric samples form different users. The threshold η defines the similarity score from which two samples are considered to be the same. An imposter score that exceeds the threshold η therefore results in a false accept, while a genuine score below the threshold η results in a false reject.

In describing the performance, different error rates are used in accordance with the international norm (ISO/IEC 19795-1:2006). The False Accept Rate (FAR) is defined as the fraction of imposters scores exceeding the threshold η. The False Reject Rate (FRR) (or, the False Non-match Rate (FNMR)) is defined as the fraction of genuine scores falling below the threshold η. The Genuine Accept Rate (GAR) is the fraction of genuine scores exceeding the threshold η and is related to the FRR by

$$GAR = 1 - FRR. \tag{1}$$

By tuning the value of η the FRR and the FAR change. It is however not possible to decrease both errors simultaneously, since a high threshold will result in a low FAR but will at the same time result in a high FRR. The opposite is true for a low threshold.

The probability density functions of the imposter and genuine scores can be estimated when a large number of scores are available. The estimates can be used to analytically derive the FAR and FRR. Let $p(s|genuine)$ and $p(s|imposter)$ represent the probability density functions of the score s under the genuine and imposter conditions respectively. For a particular threshold η the probability density functions can then be defined as

$$FAR(\eta) = \int_{\eta}^{\infty} p(s|imposter)ds, \tag{2}$$

and

$$FRR(\eta) = \int_{-\infty}^{\eta} p(s|genuine)ds. \tag{3}$$

The FAR and FRR at various values of η can be summarized using a Detection Error Tradeoff (DET) curve that plots the FRR against the FAR at various thresholds [4]. When the FAR is plotted against the GAR, a Reciever Operating Characteristic is obtained [5]. The performance of a biometric system is also often summarised using the Equal Error Rate (EER). The EER refers to the point in the DET curve where the FAR and FRR are equal. A lower EER therefore indicates better performance [2].

1.3 Biometric characteristics

Not every physical or behavioural trait is suitable for a biometric application. Jain et al. [1] identified seven characteristics that determine if a certain physical or behavioural trait could be used.

1. **Universality**: Every individual accessing the application should possess the trait.
2. **Uniqueness**: The used trait should be sufficiently different across individuals.
3. **Permanence**: In order to be a useful biometric, the trait should be sufficiently invariant over a period of time.
4. **Measurability**: It should be possible to acquire and digitize the biometric trait without causing undue inconvenience to the individual. The raw data should also be amenable to preprocessing to be able to extract representative feature sets.
5. **Performance**: The constraints imposed by the application should meet the recognition accuracy and the resources required to achieve that accuracy.
6. **Acceptability**: Individuals should be willing to present their biometric trait to the system. The user satisfaction has been shown to influence the perceived performance of a biometric system [6].
7. **Circumvention**: Circumvention refers to the ease with which the biometric trait of an individual can be imitated using artefacts and mimicry.

1.4 Types of biometric systems

There is not a single one biometric that meets all the requirements given in the section above. There are however a number of biometric traits that are admissible. The best biometric depends on the nature and requirements of the application. Below, a short introduction to the most commonly used biometric systems will be given. Since the main focus of this paper will be on iris recognition, this biometric system will be more elaborately discussed in the next section.

Face Face recognition is the most common biometric trait used by humans to recognize each other. It can also be used to automatically authenticate identity or validate identity. The two most used approaches for face recognition are based on either the location and shape of facial attributes (eyes, eyebrows, nose, lips and chin) and their spatial relationships, or on the overall analysis of the face image that represents a face as a weighted combination of a number of canonical faces [7]. There are several problems associated with face recognition, such as image degradation under poor lighting conditions and difficulties in matching faces captured under different angles [2, 8]. To solve these problems, recent research focuses on 3D face recognition and on the use of dynamic features [8,9].

Fingerprint Fingerprints have been used for identification for many years. It is based on the pattern of ridges and valleys on the surface of the fingerprint. The points where the ridge lines terminate or fork are called minutiae and are used in the classification. The most common challenge in fingerprint recognition is low quality or distorted fingerprint images due to cuts and bruises or sensor noise [10].

Hand Geometry Hand geometry recognition systems can not be used for identification, since hand geometry is not very distinctive. It can however be used for verification. Features used in hand geometry recognition include finger length, base area of the finger, area of the fingers and size of the palm [11]. Usage of hand geometry has some advantages compared with other biometrics such as being cheap, easy to use and considered as not breaching privacy. Hand geometry is however not invariant in time and jewellery and deformations due to certain diseases may pose challenges in extracting the correct information [2].

Voice When using voice as a biometric trait, physical and behavioural biometrics are combined. The physical features of an individual's voice are based on the shape and size of the appendages that are used in the synthesis of the sound. These physical aspects of speech are invariant over time in contrast to the behavioural aspects [12]. There are two different voice recognition systems: text-dependent and text-independent systems. Text-independent systems are much more complex, but provide a higher security [2].

1.4.1 Iris recognition

It is an attractive goal to be able to recognize a person in a reliable way such that the privacy of a person is not compromised. Iris recognition has a number of advantages making it an interesting biometric. First of all, iris recognition can be performed at distances of less than a meter [13, 14]. Although an individual still has to be quite close to a camera, there is no need for physical contact. Furthermore, the iris is a very unique feature, since the pattern variability among different persons is enormous. The probability of two persons having the same iris pattern is 1 to 10^{78} [15]. Even the left and right iris differ from each other. Additionally, the iris is well protected from the environment and stable over time. However, it degenerates quickly after death and can thus not be used to identify dead bodies [15]. Another advantage of the iris as a biometric is the fact that it is quite easy to localize the iris in face images. The annular shape of the iris facilitates a reliable and precise isolation of this feature and the creation of a size invariant representation [14]. For all these reasons, iris recognition is an attractive biometric trait to reliably identify of verify identity.

The iris starts forming in the third month of gestation, the pattern is complete by the eight month [16]. Its complex can contain many distinctive features such as arching ligaments, furrows, ridges, crypts, rings, corona, freckles and a zigzag collarette [17]. The forming of iris depends on the initial environment of the embryo, so the iris texture patters do not correlate with genetic determination. The predominant structure seen under visible light is created by the striated trabecular meshwork of elastic pectinate ligament. In the near-infrared wavelengths, often used for unobtrusive imaging at distances of up to 1 m,

deeper and more slowly modulated stroma features are visible in the iris pattern. Darkly pigmented irises reveal rich and complex structures when imaged with near-infrared light [14].

The accuracy of iris recognition systems is proven to be much higher compared to other types of biometric systems like fingerprint, handprint and voiceprint. Some of the results of previous work on iris recognition are listed in Table 1 [18]:

Group	**Size of Database**	**Results**
Daugman	4258	EER=0.08%
Wildes et all	60	EER =1.76%
Li Ma	2245	Correct Recognition Rate =94.33%

Table 1: Results gained from previous research.

A typical iris recognition system consist of four main modules: image acquisition, preprocessing, feature extraction and comparisons with existing stored patterns. The image acquisition deals with capturing sequence of iris images from the subject using cameras and sensors. Preprocessing involves various steps such as pupil and iris detection, eyelid removal and normalization. Feature extraction identifies the most prominent features for classification. The last module compares irises with the stored irises.

2 Theoretical background

2.1 Preprocessing

2.1.1 Pupil detection

For an iris recognition system the first important step is to find a pupil in the image. The pupil of a human has a circular shape and appears to be black. To find a pupil a circular edge detection can be performed. One way to do this is to use [17] :

$$max\ |G_\sigma(r) * \frac{\partial}{\partial r} \oint_{r,x_0,y_0} \frac{I(x,y)}{2\pi r}|, \tag{4}$$

where $I(x,y)$ is an image containing an eye. The operator searches over the image domain (x,y) for the maximum in the blurred partial derivative with respect to increasing radius r and the center coordinates. It fits a circle with radius r and starting point x_0 and y_0 and calculates the gradient. The pupil is located at the maximum value of the gradient. $G(r)$ is a radial Gaussian function with center r_0 and standard deviation σ that smooths the image to select the spatial scale of edges under consideration.

Another way to find the pupil is to apply an edge detection to the image. The pupil is very black in comparison with everything else in the picture, so an edge detection should be able to find its outside edge very easily. Canny edge detection [19] can be used since this algorithm uses horizontal and vertical gradients in order to deduce edges in the image. To clean up the image one can dilate all the edge detected lines to give a higher probability that the perimeter of the pupil is a complete circle. By computing the euclidean distance from any non-zero point to the nearest zero valued point an overall spectrum can be found. This spectrum shows the largest filled circle that can be formed within a set of pixels. Since the pupil is the largest filled circle in the image the overall intensity of this spectrum will peak here. The pupil center will have the highest value. The value at that maximum (distance from that point to the nearest non-zero) must be equal to the pupil radius. [20]

2.1.2 Iris detection

The same method as described in section 2.1.1 can be used to detect the iris. Again, the following equation is used:

$$max\ |G_\sigma(r) * \frac{\partial}{\partial r} \oint_{r,x_0,y_0} \frac{I(x,y)}{2\pi r}|, \tag{5}$$

only now to find the iris instead of the pupil. Additionally, a certain offset in the radius is used to find the edge between the iris and the sclera.

The system developed by Wildes et al [21] performs its contour fitting in two steps. First the intensity of the image is converted to binary edge-map. Thereafter, edge points vote to instantiate particular contour parameter values. The edge map is recovered via gradient-based edge detection. This operation consist of thresholding the magnitude of the image intensity gradient. This is done with $G(x,y) = *I(x,y)$ whereby G(x,y) is the same radial function as Daughman [13] uses. In order to incorporate directional tuning, the image intensity derivatives are weighted to favour certain ranges of orientation prior to

taking the magnitude. The voting procedure is realized via Hough transforms on parametric definitions of the iris boundary contours. A hough transform is defined as:

$$H(x_c, y_c, r) = \sum_{j=1}^{n} h(x_j, y_j, x_c, y_c, r) \tag{6}$$

where

$$h(x_j, y_j, x_c, y_c, r) = \begin{cases} 1, \text{if } g(x_j, y_j, x_c, y_c, r) = 0 \\ 0, \text{otherwise} \end{cases} \tag{7}$$

with

$$g(x_j, y_j, x_c, y_c, r) = (x_j - x_c)^2 + (y_j - y_c)^2 - r^2. \tag{8}$$

For each edge point this g will be zero for every parameter triple (x_c, y_c, r) that represents a circle trough a point. Correspondingly, the parameter triple that maximizes H is common to the largest number of edge points and is a reasonable choice to represent the contour of interest.

The iris is surrounded by the white sclera and the pupil. The most easy way to find the iris is to filter with a Haar wavelet. A Haar wavelet has a orthogonal base of block-like functions and it can be used to detect edges. When selecting a row of pixels starting at the outer radius of the pupil to the right of the eye, an edge would be expected at the boundary of the iris with the white sclera. Here pixel values differ the most from each other. When applying the Haar wavelet, one calculates the average between two pixels and then it determines the distance between the second pixel and the average. When two pixel values differ very much this second number will be big. Therefore, Haar wavelets can be used to detect the boundaries of the iris [15, 20].

2.1.3 Iris normalization

After the position of the iris and pupil are determined, the unwrapping of the iris can be performed. The unwrapping of the iris involves the process of converting the Cartesian coordinate system into a polar coordinate system. This method is performed after histogram normalization is applied.

In 2005 B.J. Joung [22] described three different methods for unwrapping the iris. The first method is to assume that the mean center of the iris is positioned at the mean center of the pupil. Although this is a straight forward assumption, it does result in not considering the iris center coordinate and its radii. This results in information loss because the iris region is subject to change due to variables of light or illumination.

A second method which Joung describes, is to determine the center and contours of both the pupil and the iris, as shown in Figure 1. From the pupils center (Cp) two points ($p1$ and $p2$) on the outline of the pupils are determined, with an angle of $d\theta$ in between. In a similar way two points ($p3$ and $p4$) are determined on the outer edge of the iris using the center point and radius of the iris. The created wedge is segmented using circles with Ci as a center, shown in yellow. De segment is the averaged and plotted against r and θ axis.

The third method described by Joung is similar to the second one. Joung argues that the most valuable information of the iris is located in the centre. Thus he concludes that only the inner 50% of the iris should be unwrapped.

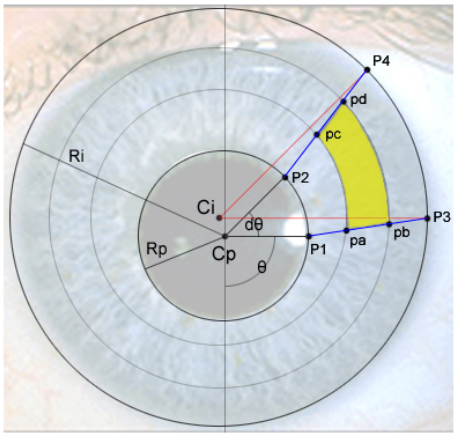

Figure 1: Segmentation for unwrapping of the iris using the centre of the iris and pupil. Figure adapted from [20].

2.1.4 Eyelid removal

There are several ways to detect the eyelids. Daughman [17] uses the same method as he uses to detect the pupil and the iris, but now the path of contour integration is changed from circular to evacuate, with spline parameters fitted by statistical estimation methods to model each eyelid boundary. If the iris is covered by eyelids and eyelashes for more than 50% the image is discarded.

Another not so delicate method is to throw away the bottom part of the image. This way a lot of information is lost.

Wildes [23] uses a gradient-based edge detector that is tuned in the horizontal orientation. The upper and lower eyelids are modelled as (two separate) parabolic arcs with the form $x(t) = a_x t^2 + b_x t + c_x$ and $y(t) = a_y t^2 + b_y t + c_y$ with $0 \leq t \leq 1$ and parameters to be fit $a_x, b_x, c_x, a_y, b_y, c_y$.

2.2 Feature extraction

Once the iris image is transformed to the polar coordinate system, features should be extracted for classification. The most common used feature extraction method in iris recognition is the use of Gabor filters, as suggested in Daugmans paper [17]. Daugman suggests to use a quadrature 2-D Gabor wavelet for filtering and decode the resulting image, using the real and imaginary part. This will be described in more detail in section 2.2.3. Other used methods for iris recognition are 1-D intensity signals [24] and a zero crossing wavelet transform [25].

2.2.1 1D intensity signals

Another method to extract the features of the iris is described in the paper of Li Ma [24]. This method uses 1-D intensity signals. The position of local sharp variation points are recorded as features. The information density is much higher in the horizontal direction of the normalized image than in other directions, therefore it is sufficient to only capture local shape variations in this

direction to characterize an iris. They decompose the 2D normalized image I into a set of 1D intensity signals S according to the following equation:

$$s_i = \frac{1}{M}\sum_{j=1}^{M} I_{(i-1)*M+j} \qquad i = 1, 2, ...N, \tag{9}$$

$$I = \begin{pmatrix} I_1 \\ . \\ . \\ . \\ I_x \\ . \\ . \\ . \\ I_k \end{pmatrix} = (I_1^T, ..., I_x^T, ..I_k^T)^T, \tag{10}$$

where I is the normalized image of $K * L$. I_x denotes grey values of the x-th row in the image, M is the total number of rows used to form a signal S_i, N is the total number of 1-D signals. In essence, each intensity signal is a combination of M successive horizontal scan lines which reflect local variations of an object along the horizontal direction.

2.2.2 Zero crossings wavelet transform

The iris recognition method, using the zero crossings wavelet transform, is proposed by Boles and Boashash in 1998 [25]. They first extract the pupil and iris location. Thereafter they define circular shapes on the iris area. The circular shapes are defined such that they are not influenced by the recorded diameter of the iris and thus represent the same iris area in every iris image. On these circles N sample points are chosen, such that the accuracy is high enough, but the data does not become too large. For these circular sampled iris wavelets, the zero crossings are calculated. Because the patterns represent a closed ring, it will be periodic with N and the starting point will not influence the total outcome. For matching two iris images, these circular zero crossings patterns will be compared. The patterns will be shifted and compared and the minimum distance will be saved as error value. This is done for every circular zero crossing pattern. The error value can be used in a classifier. This method is translation and size invariant [25], but got a higher EER than other systems [18].

2.2.3 Gabor wavelet

A Gabor wavelet consists of a harmonic function modulated with a Gaussian window function [26]. For feature extraction, convolution with a quadrature pair of Gabor filters is used [27]. The real part of the quadrature pair consists of a cosine modulated by a Gaussian, the complex part contains a sine wave modulated by a Gaussian. The bandwidth of the filter is specified by the width of the Gaussian envelope, the center frequency by the frequency of the sine and cosine wavelets. A 2D Gabor filter is represented as [13]:

$$G(x, y) = e^{-\pi[\frac{(x-x_0)^2}{\alpha^2}+\frac{(y-y_0)^2}{\beta^2}]} * e^{-2\pi i[u_0(x-x_0)+v_0(y-y_0)]}, \tag{11}$$

where (x_0, y_0) specifies the center position of the filter in the image, (α, β) specifies the effective width and length and (u_0, v_0) specifies the modulation frequency $\omega_0 = \sqrt{u_0^2 + v_0^2}$ and the direction $\theta_0 = arctan(\frac{v_0}{u_0})$. A 1D and 2D example of a Gabor filter in the time / image domain, are shown in Figure 2.

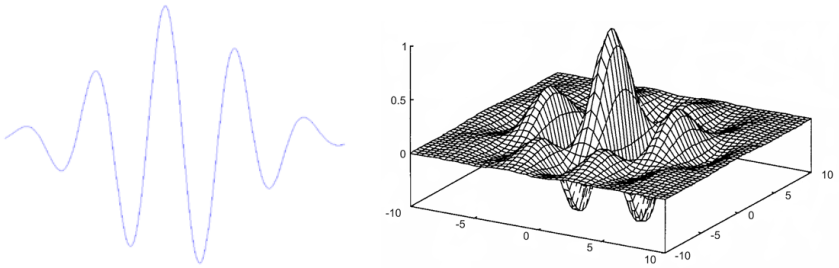

Figure 2: Examples of Gabor functions (real parts) [28], [29].

The Fourier transform of this 2D Gabor function is [13]:

$$F(u, v) = e^{-\pi[(u-u_0)^2\alpha^2 + (v-v_0)^2\beta^2]} * e^{-2\pi i[x_0(u-u_0) + y_0(v-v_0)]}. \quad (12)$$

An example of a 2D Gabor function in the image domain and its Fourier transform are shown in Figure 3 [13]. As expected, the frequency response shows a peak at a certain frequency and it has a certain orientation. When filtering an image with this Gabor wavelet, the image properties for that frequency and orientation are obtained. Using multiple frequencies and orientations, features could be extracted out of the images.

2.2.4 Iris code

After filtering the iris image with a Gabor filter, the dimensionality of the image is still the same. Therefore the Gabor filtered image is decoded in a so called iris code [13]. It uses the phase information of the filtered image to decode the iris image in grey code, as shown in Figure 4. The advantage of using only phase information is that it is less influenced by image contrast, illumination and camera properties [17]. The advantage of the grey code is that it is less error sensitive [17].

2.3 Matching algorithms

After the feature vector is obtained and before classification can take place, the feature vectors are compared. The obtained feature vectors can be seen as binary codes. There are several comparison methods, but the common used method in iris recognition is the Hamming distance.

2.3.1 Hamming distance

The Hamming distance is a measure of the dissimilarity between two bit patterns. It counts the amount of unequal bits between two bit patterns, using an

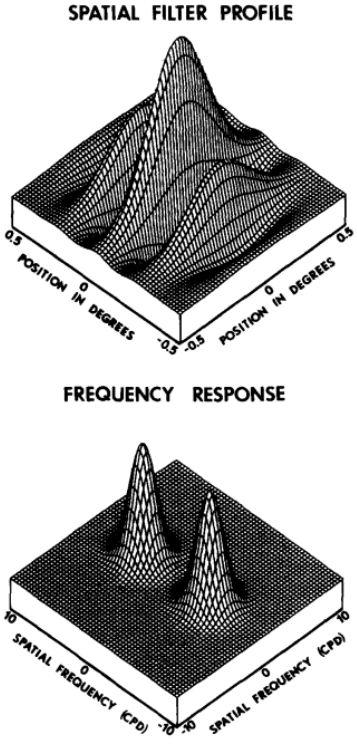

Figure 3: Real part of a 2D Gabor function and its Fourier transform [13].

exclusive OR ($\oplus$):

$$HD = \sum_{j=1}^{N} X_j \oplus Y_j \tag{13}$$

with X and Y the two bit patterns and j the index.

In this case the whole iris image is compared, which contains still the eyelid parts. Therefore the masker images should also be taken into account, by ANDing ($\otimes$) the iris images with the masks. After masking the images, the size of the images is different and therefore the computed Hamming distance should be normalized by dividing by the size of the image:

$$HD_{norm} = \frac{\sum_{j=1}^{N}((X_j \oplus Y_j) \otimes (mask_X \otimes mask_Y))}{size(mask_X \otimes mask_Y)}. \tag{14}$$

The normalized Hamming distance is thus a measure of dissimilarity between two iris images, with a value between 0 (equal) and 1 (totally different). For two uncorrelated iris images this distance has an expected value of 0.5. Daugman [14] calculated the Hamming distance for about 9 million comparisons of uncorrelated pairings of iris images, and calculated their distribution (see Figure 5). The observed mean was 0.499 and the standard deviation $\sigma = 0.0317$, which confirms the expected value of 0.5.

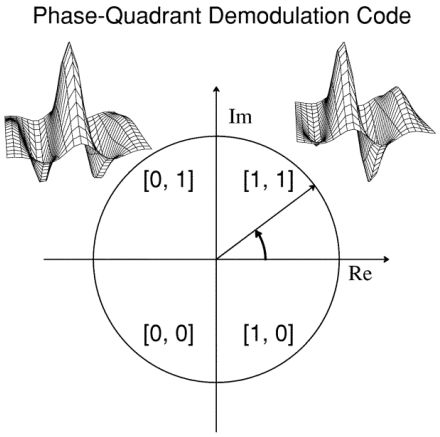

Figure 4: Using phase information to decode the iris image. The phase information is decoded in four quadrants, resulting in two bits of information.

2.3.2 Orientation compensation

The iris images of the same persons can have a different orientation, which makes the classification more difficult. When this rotation is not compensated for, the wrong iris regions are compared. To compensate for the orientation error, multiple shifted versions of one of the images are compared. In that case the iris code is shifted a few times two bits to the left and a few times two bits to the right. All these versions are compared with another iris code. The best match (lowest HD) is the used score for the classification. For iris codes of the same iris, the classification probably improves. For iris codes of different irises, the classification is affected less, because these images are uncorrelated and the expected HD is around 0.5.

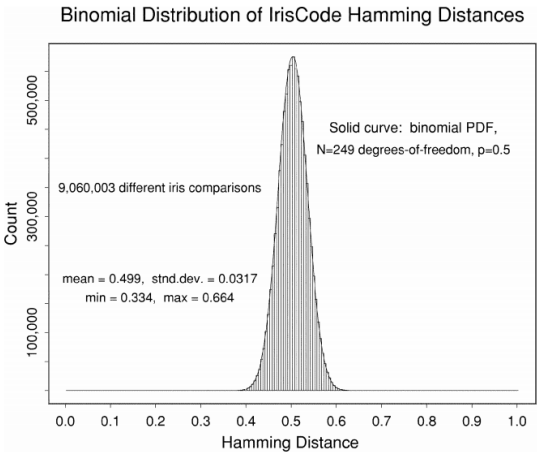

Figure 5: Distribution of Hamming distances from about 9 million comparisons between different pairs of iris images.

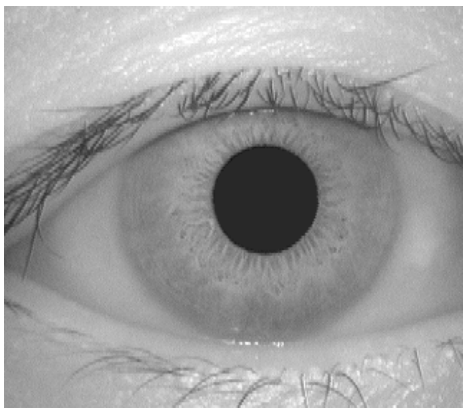

Figure 6: Iris image from the CASIA database [30].

3 Methods

3.1 Data acquisition

To develop and test the proposed iris recognition system, the CASIA iris database version 1.0 is used [30]. The CASIA database is free to use and is provided by the Chinese Academy of Sciences to promote research into iris recognition. The images are captured with a home made iris camera with eight 850 nm near infrared (NIR) illuminators circularly arranged around the sensor to illuminate the iris uniformly. The pupil regions of all iris images are automatically detected and replaced with a circular region of constant intensity to mask out the specular reflections from the NIR illuminators before the images are stored in the database.

The database consists of 756 iris images from 108 eyes. For each eye, seven images are captured in two sessions. Three samples are collected in the first session and four in the second session. All images are stored as BMP format with a resolution of 320 by 280 pixels [30]. Figure 6 shows an example of an iris image in the CASIA database. In the development of the system described in this report, the images of ten individuals (a total of seventy images) are used as a training set. The remaining 686 images are used as the test set.

3.2 Preprocessing

3.2.1 Pupil detection

To detect the pupil, Canny edge detection [19] is used and the result of this edge detection is slightly dilated so that the probability that the perimeter of the pupil is complete is higher. All closed regions are then filled and small objects are removed, so that only the pupil remains. The image is then complemented and the Euclidean distance is computed. The Euclidean distance computes the distance from any non-zero point to the nearest zero value point. When we assume that the pupil is circular, the pixel with the highest value will be the center of the pupil and the value at that maximum, which is the distance to the

nearest zero valued point) will be the radius of the pupil. This is a fairly easy and quite robust method to find the pupil, requiring low processing power.

3.2.2 Iris detection

The iris is detected using Haar wavelets. Two different methods are used.

Since the center of the iris is often not the same as the center of the pupil, the Haar wavelet is used in three directions to be able to determine the center and radius of the iris. A row of pixels is selected and filtered with a Haar wavelet. The maximum of the response is the position of the border of the iris. The three directions used are horizontal to the left, horizontal to the right and under an angle of 26 degrees to the right bottom corner. All rows have the pupil center with a certain offset greater than the radius of the pupil as a starting point. The last few pixels of the row are ignored, since this could contain eyelids. The eyelid-sclera boundary gives a greater response to the Haar wavelets than the iris-sclera boundary, so the eyelid-sclera boundary should not be included. From each direction a maximum is found and this location is used to draw a circle using three points. This circle has a center which equals the iris center and the radius is the radius of the iris.

Another method used is using two points and using the center of the pupil. The pixel row to the left and right of the pupil center are filtered and the maximum value position is determined. From these two points the radius can be determined assuming that the pupil center is the same as the iris center. This method is used instead of a three point method in case that in many images the eyelid is detected as third point which causes an invalid circle to be drawn. However the first method will find the iris with more accuracy because the iris center and the pupil center are not always the same.

3.2.3 Iris normalization

As described in Section 2.1.3, three main methods can be used to normalise the iris. Joung [22] states that the cropped version has a higher matching rate than the normal version of the Doubly polar method. A second advantage of the cropped method is that it uses less bits of data. Both methods will be tested in this project and the resulting EER will be compared. This is done because it is hypothesised that the recognition system needs as much information as possible, since it might not be accurate enough to work with less information.

In the Doubly polar method, the lines $p1p3$ and $p2p4$ have been determined as described in Section 2.1.3 and as can be seen in Figure 1. Along these lines 22 points have been defined, the angle θ is chosen to be $1.2°$. These have been empirically determined in order to create adequate distances in between the points, taking in account the size of the pixels of the images. Each pair of four points form a surface area, which is determined by the function *inpolygon*. As an input a grid has been given, with the pixel coordinates of the original image. The function outputs the positions of the pixels included in the area. Over these pixels the mean is taken and transposed to a Cartesian image.

Exactly the same method is used for the cropped version of the Doubly polar method, except only the inner 50% of the iris is used in unwrapping.

3.2.4 Mask creation

The unwrapped iris image still contains some parts that need to be discarded when comparing the image with another iris. This is due to eyelashes and eyelids covering the iris. Therefore, a binary mask is created, indicating which pixels have to be taken into account in the recognition part of the system.

Eyelashes and eyelids have quite strong edges with the iris. Therefore, canny edge detection [19] is used to detect the boundaries of the eyelids and the eyelashes. The detected boundaries are then dilated a bit so that the eyelids, which appear as halve circles, become closed and can be easily filled. The image is then complemented, so that pixels with useful information get index one and pixels with non-useful information (eyelids and eyelashes) get index zero. The zero's are then converted to NaN to give them no influence in the recognition part.

3.3 Feature extraction

3.3.1 Gabor filter and iris code

For the feature extraction Gabor filters are used and thereafter an iris code is extracted. The unwrapped iris image is filtered with four Gabor filters, each with a different orientation. The orientation differs from 0 radians to $\frac{3}{4}\pi$ radians, thus four orientations in the range from 0 to π. Only the range from 0 to π is used, because the range from π to 2π results in the same images, but inverted and thus contains the same information. The aspect ratio is set at 0.5 and the bandwidth at 2. The wavelength is chosen at 6, which is about one period of the patterns in the unwrapped images. The four Gabor filtered images are decoded into iris code images, using the phase of the filtered images. The phase is decoded in four quadrants, each two bits, which are grey coded.

3.4 Matching

3.4.1 Hamming distance

For the verification of two iris images, a matching score is needed. In this case the Hamming distance is used, as proposed by Daugman [14]. For both iris images the four filtered images are masked with masks of both iris codes, to avoid comparison of non iris parts. Thereafter the Hamming distance is calculated for all these four filtered images and added up. One of the images is shifted ten times two pixels to the left and to the right. For each of these shifted versions the Hamming distance is calculated and the minimum of these distances is used as dissimilarity measure. In this case the best match between the two templates is chosen and the influence of rotation is reduced. A threshold (linear classifier) on these distances is used for calculating the ROC curve and the EER.

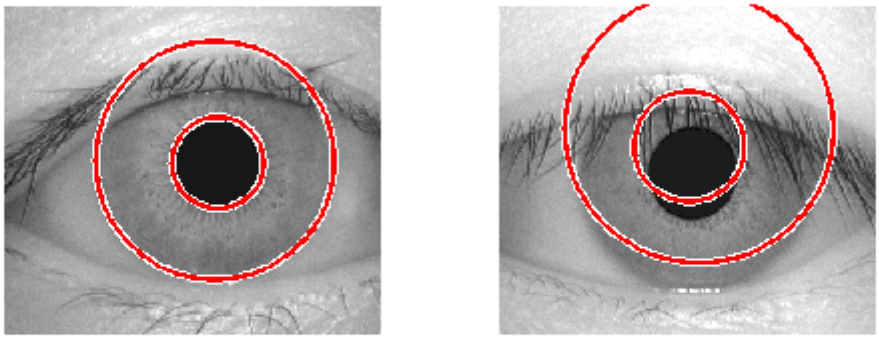

Figure 7: a) A well detected pupil. b) A bad detected pupil.

4 Results

4.1 Preprocessing

4.1.1 Pupil detection

The training set has been analysed to test the pupil detection algorithm. The pupil detection algorithm detects 67 out of 70 images correct. An example of a good and bad detected pupil can be seen in Figure 7. As can be seen, when the pupil is not detected correctly, the iris is also not detected correctly.

4.1.2 Iris detection

Two methods of iris detection have been analysed on the training set. The first method uses two point circle detection and 65 out of 70 irises are detected correct. When using the three point method 58 out of the 70 irises are detected correctly. An example of a good and bad detected iris can be seen in Figure 8. An example of iris detection using the three point method can be seen in Figure 9.

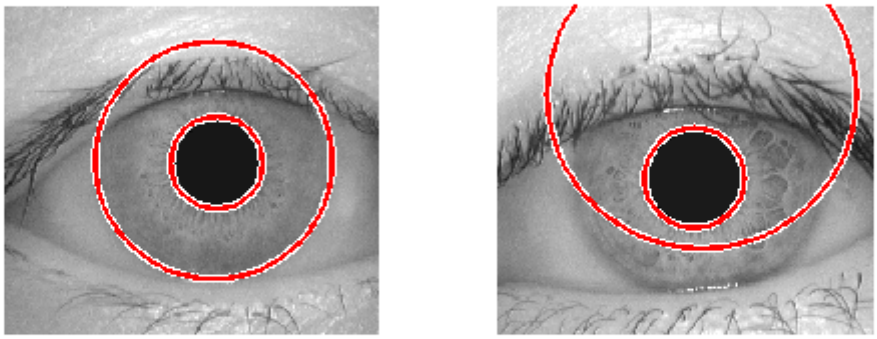

Figure 8: a) A well detected iris. b) A bad detected iris.

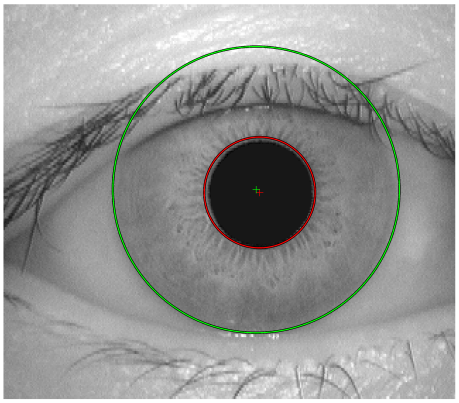

Figure 9: Example of an eye with the border of the pupil in red and the border of the iris in green. The center of the pupil is indicated with a red +, the center of the iris is indicated with a green +.

Figure 10: The result of normalizing the iris and creation of the mask.

4.1.3 Iris normalization

All irises are normalized. A result of this can be seen in Figure 10. The upper part shows a normalized iris in which clearly the eyelids and eyelashes can be seen.

4.1.4 Mask creation

A mask has been created to remove the eyelids and eyelashes. The lower part of Figure 10 shows the result of the eyelid removal. The upper image shows the unwrapped iris. It can be seen that there are still eyelids present in the image. The lower figure shows the mask corresponding to the unwrapped image. The black parts are the parts that will not be taken into account in the recognition part. Masks that consist of more than 50% of NaNs will not be taken into account in the recognition part, since there is not enough iris left to make a reliable comparison.

4.2 Feature extraction

The resulting iris code images have a size of 22 x 600 x 4. An example of a decoded iris image is shown in Figure 11. The iris code images are obtained by using a gabor filter in four directions.

4.3 Matching results

The implemented system is evaluated, using the training and test set. For each set a ROC curve is made and the EER is calculated. Different implementation versions are tested and the results are presented for every method.

The first method uses a simple iris detection method, which uses only two points. The ROC curve of the test set is shown in Figure 12. This method results in an EER of 0.0913. In total 74 images failed to enrol, which is about 10.8% of the total dataset, containing the images from which more than 50% of the unwrapped iris is masked out. The EER for evaluating the training set

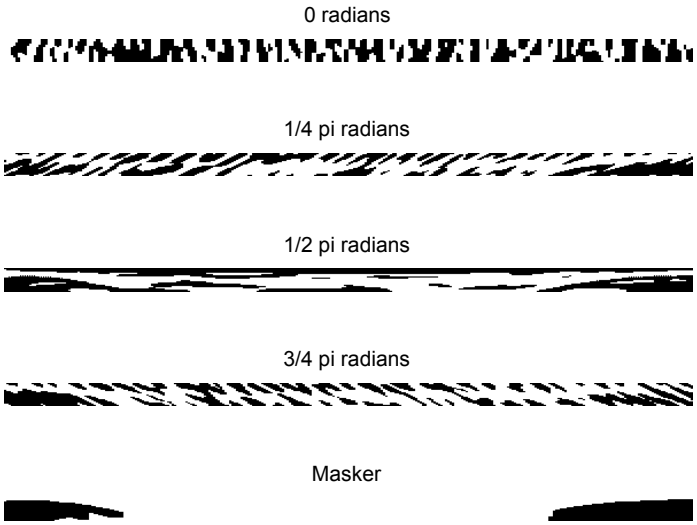

Figure 11: Example of an iris decoded image.

Method	EER Training set	EER Test set	Failure to Enrol
Two point iris detection	0.1264	0.0913	10.8%
Three point iris detection	0.1660	0.2342	6.7%
Lower half of iris (two point detection)	0.1092	0.0762	6.7%

Table 2: Results of iris recognition systems using different methods.

is 0.1264. The total processing time, using a normal computer, was about 4.5 hours.

The system is also tested for a more complex iris detection methods, using three points. This methods makes it possible to relocate the center of the iris, instead of mapping it onto the center of the pupil. This system is also evaluated on the test and training set, resulting in an EER of 0.2342 and 0.1660 respectively. The ROC curve for the test set is shown in Figure 13. For this system the failure to enrol is about 6.7 %.

Joung [22] proposes a method for normalizing the iris image, in which only the inner 50 % of the iris is used. In the script used, the outer 50% of the iris is removed by removing half of the unfolded iris after masking. This has been performed in order to the test if this method is more efficient, without the results being influenced by the subscript responsible for masking the unfolded iris. This method is also implemented and tested, using the simple iris detection. This results in the ROC curve in Figure 14 and an EER of 0.0762 for the test set and 0.1092 for the training set. A histogram of the impostor and genuine scores is shown in Figure 15. The failure to enrol for this implementation is 6.7 %. If only the inner 50% of the iris would be unfolded, it is estimated that this method would take about 3 hours. This estimation is based on a profile summary made of this method.

An overview of all results is presented in Table 2. Also the failure to enrol of the test set is given in this table.

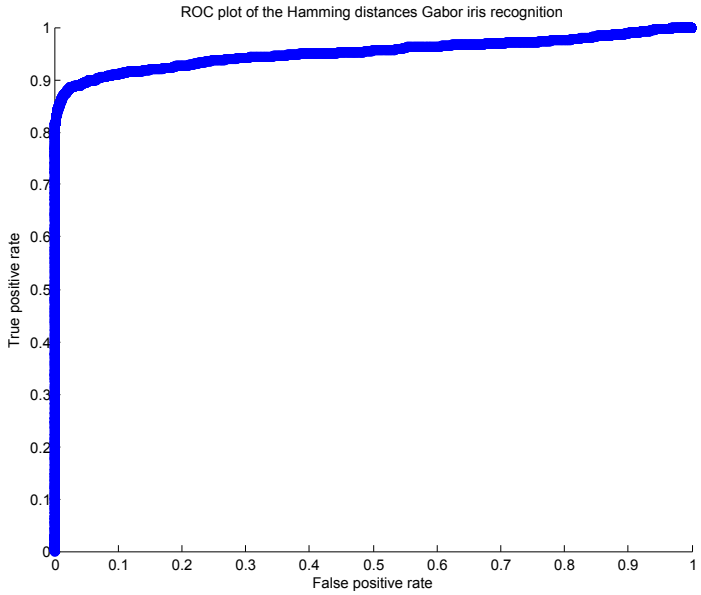

Figure 12: ROC curve of the method with simple iris detection of the test set.

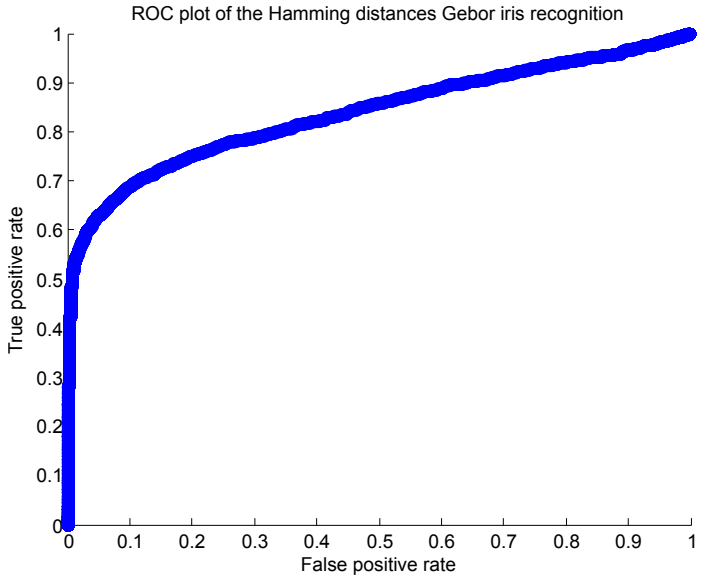

Figure 13: ROC curve of the method with iris detection using three points.

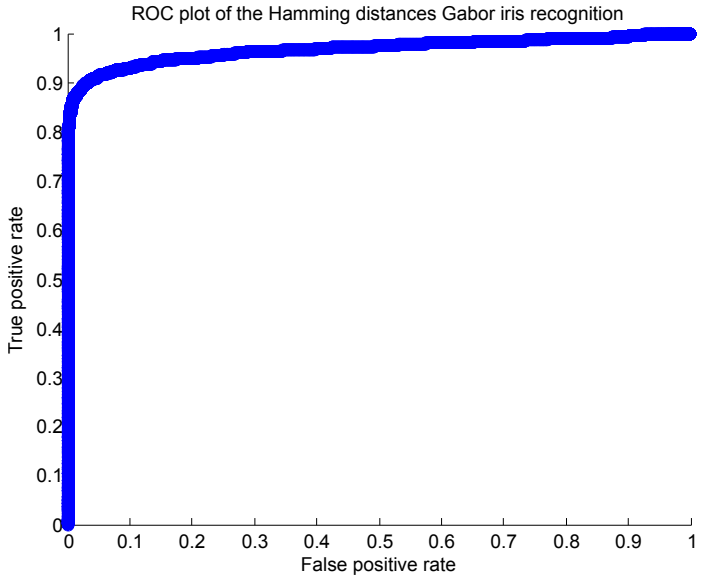

Figure 14: ROC curve of the method using 50% of the iris.

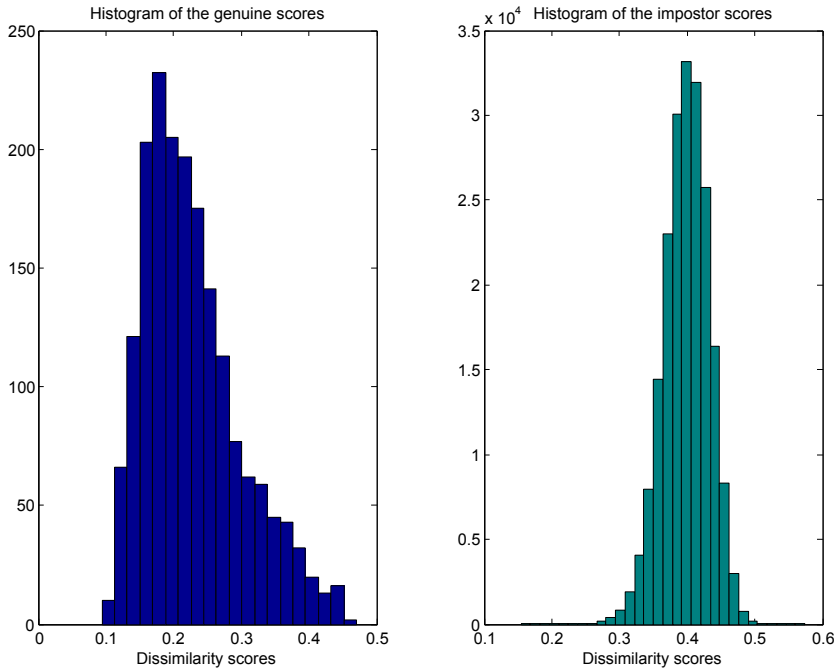

Figure 15: Histogram of the genuine and impostor scores for the method using 50% of the iris.

5 Discussion

The three designed systems are tested, using a training and test set. From the results (see Table 2) it can be concluded that the iris detection method using only two points gives the best result. For the simple iris detection method, the EER on the training set is higher then on the test set, probably because of the small size of the training set. When only 50 % of the iris area is used, the EER increases with 1.5 % and the failure to enrol decreases with 4 %. In that case the processing time could be reduced by 25 %. Reducing the used region of the iris with 50 % improves thus the performance of the system, probably because the regions of the eyelids are filtered out more effectively. The iris detection method using three points, decreases the performance drastically, resulting in a EER of 0.2342. This is due to the fact that the eyelid is detected instead of the border of the iris with the sclera.

It might be good to look again at the method using three points to detect the iris. This has to be implemented such that the eyelid is not found but an other border of the iris with the sclera. The system might be improved by using the improved three point detection system and using the 50% method to remove most of the noise.

When looking at the histogram of the impostor scores (see Figure 15), it can be seen that the dissimilarity scores are centred around 0.4, with a variance of 0.0011 and the expected Gaussian shape. It was expected that the scores would be centred around 0.5, because the images are uncorrelated. The genuine scores have a mean of 0.2277 and a variance of 0.0051. A part of the scores overlap with the impostor scores, but most of the scores could be separated well.

The proposed system is currently trained and tested on the CASIA database version 1.0 [30] only. This database consists of even illuminated eyes without specular reflections. Also, the eyes are already segmented from the face and a near-infrared camera is used. All parameters used in the system are now set to the images in this database and should be adjusted when the system is tested on other databases. The performance of the system on other databases will therefore probably be less.

Some mistakes are made when detecting the pupil and the iris. Looking at the training set, there are three eyes where the pupil is not detected correctly. In all these eyes, the eyelashes are hanging down over the pupil. When applying edge detection, the pupil is not correctly segmented from the eyelashes and the center and radius will not correspond to the real center and radius. The method as proposed by Daugman [17], in which a circle is fitted, will probably give better results at these images. However, this method is also computationally more intensive.

Two different methods of iris detection are tested. The first method uses two points to find the iris. This method assumes that the center of the iris is the same as the center of the pupil. The other method uses three points to fit a circle to the iris. The advantage of this method is that the center of the iris does not need to be the same as the center of the pupil. The performance of this method is however less than the method with only two points. This is mainly because the third edge point is often located at the eyelid boundary. Furthermore, in selecting the rows of pixels on which the Haar wavelet is used, it is still assumed that the pupil center and iris center are the same. Both methods have difficulties in finding the iris when the iris contains very clear spots. These

spots probably have a higher contrast than the iris-sclera boundary. This could be solved by assuming a minimal radius of the iris, since these spots are often close to the pupil. When a boundary point is found too close to the pupil, the second highest response to the Haar wavelet should be taken, since this will then be the iris-sclera boundary.

In unwrapping the iris, a surface is created in between each four points of which the mean is taken. The value found is then transposed to a Cartesian image. By using the function *inpolygon* a square area between the coordinates is created, instead of taking in the curvature of the radius into account. Because the areas that are created are so small, the curvature can be neglected. Furthermore, the number of radii and angle in between the outward lines have been determined empirically. Although it is assumed this is best compatible with the current system, further experimenting with these parameters might eventually result in a lower EER.

The performance of the system could be further improved by improving the masking method. At this moment, the mask primarily finds the eyelids and only in some cases the eyelashes. This is due to the fact that the mask is made using edge detection. The parameters of the edge detection are set to only finds strong edges to limit the need for post-processing. As a consequence, the less strong edges of the eyelashes are not found. By adjusting the parameters of the edge detection, the eyelashes could also be found. However, this requires a lot more post-processing, since also many spurious edges will be found.

The parameters used for the Gabor filter are empirically determined. In the proposed system, four different orientations are used. More orientations will probably not contain much more information and will increase the computation time. The used wavelength and aspect ratio should be chosen such that a few periods of the pattern are enclosed by the Gaussian. Better results might be obtained when the different parameters are systematically tested.

To reduce the influence of rotation, the irises are shifted ten times two pixels to the left and to the right. This will compensate for the small rotations present in the database used. However, when more rotation is present, a shift over the whole image might be needed to compensate for the rotation. This will however increase the computational time.

The proposed method uses the Hamming distance to match the irises. Although this is a widely accepted method in iris recognition, better results might be obtained when using a non-linear classifier such as a quadratic classifier. When using the Hamming distance, all features are given equal weight. However, most of the information is in the horizontal direction. It could thus be beneficial to give this feature a larger weight when comparing the irises.

6 Conclusion

Different methods have been tested for the proposed iris recognition system. As can be seen in Table 2 the best score is obtained when only the inner half of the iris is used. In this method the iris is detected using a two point algorithm. With this method an EER of 0.0726 is obtained using 686 images of 98 people from the CASIA version 1.0 database [30]. Of these 696 images, 46 failed to enrol using this method. In the discussion advantages and disadvantages using our methods are discussed. Recommendations can be derived for the future

development of iris recognition systems.

7 Bibliography

[1] A. K. Jain, R. M. Bolle, and S. Pankanti, *Biometrics: personal identification in networked society*. Springer, 1999.

[2] A. Ross and A. K. Jain, "Human recognition using biometrics: an overview," in *Annales Des Télécommunications*, vol. 62, pp. 11–35, Springer, 2007.

[3] N. Clarke and S. Furnell, "Biometrics the promise versus the practice," *Computer Fraud & Security*, vol. 2005, no. 9, pp. 12 – 16, 2005.

[4] A. Martin, G. Doddington, T. Kamm, M. Ordowski, and M. Przybocki, "The det curve in assessment of detection task performance," tech. rep., DTIC Document, 1997.

[5] J. A. Swets, *Signal detection theory and ROC analysis in psychology and diagnostics: Collected papers*. Lawrence Erlbaum Associates, Inc, 1996.

[6] M. El-Abed, R. Giot, B. Hemery, and C. Rosenberger, "A study of users' acceptance and satisfaction of biometric systems," in *Security Technology (ICCST), 2010 IEEE International Carnahan Conference on*, pp. 170–178, IEEE, 2010.

[7] S. Z. Li and A. K. Jain, *Handbook of face recognition*. springer, 2011.

[8] A.-M. Moore, "Biometric technologiesan introduction," *Biometric Technology Today*, vol. 15, no. 1, pp. 6–7, 2007.

[9] A. Hadid, J.-L. Dugelay, and M. Pietikäinen, "On the use of dynamic features in face biometrics: recent advances and challenges," *Signal, Image and Video Processing*, vol. 5, no. 4, pp. 495–506, 2011.

[10] A. Singhal and V. Mittal, "A brief review: Fingerprint authentication system," *International Journal of Applied Engineering Research*, vol. 7, no. 11, 2012.

[11] A. Plichta, T. Gaciarz, and S. Szomiński, "Identification of persons by virtue of hand geometry," in *Computer Information Systems and Industrial Management*, pp. 36–46, Springer, 2013.

[12] J. P. Campbell Jr, "Speaker recognition: A tutorial," *Proceedings of the IEEE*, vol. 85, no. 9, pp. 1437–1462, 1997.

[13] J. G. Daugman, "High confidence visual recognition of persons by a test of statistical independence," *IEEE Transactions on pattern analysis and machine intelligence*, vol. 15, pp. 1148–1161, November 1993.

[14] J. Daugman, "The importance of being random: statistical principles of iris recognition," *Pattern recognition*, vol. 36, no. 2, pp. 279–291, 2003.

[15] R. Veldhuis, "Introduction to iris recognition," *University of Twente*, October 2013.

[16] P. Kronfeld, "Gross anatomy and embryology of the eye," *The eye*, vol. 1, pp. 1–66, 1962.

[17] J. Daugman, "How iris recognition works," *IEEE transactions on circuits and systems for video tehcnology*, vol. 14, pp. 21–30, January 2004.

[18] S. Sheela and P. Vijaya, "Iris recognition methods- survey," *International Journal of Computer Applications*, vol. 3, no. 5, 2010.

[19] J. Canny, "A computational approach to edge detection," *Pattern Analysis and Machine Intelligence, IEEE Transactions on*, no. 6, pp. 679–698, 1986.

[20] D. Khabashesku, "Iris recognition," 2004. http://cnx.org/content/col10256/1.1/.

[21] R. P. Wildes, "Iris recognition: an emerging biometric technology," *Proceedings of the IEEE*, vol. 85, no. 9, pp. 1348–1363, 1997.

[22] B. J. Joung, C. H. Chung, K. S. Lee, W. Y. Yim, and S. H. Lee, "On improvement for normalizing iris region for a ubiquitous computing," in *Computational Science and Its Applications–ICCSA 2005*, pp. 1213–1219, Springer, 2005.

[23] R. P. Wildes, J. C. Asmuth, G. L. Green, S. C. Hsu, R. J. Kolczynski, J. Matey, and S. E. McBride, "A system for automated iris recognition," in *Applications of Computer Vision, 1994., Proceedings of the Second IEEE Workshop on*, pp. 121–128, IEEE, 1994.

[24] L. Ma, T. Tan, Y. Wang, and D. Zhang, "Efficient iris recognition by characterizing key local variations," *Image Processing, IEEE Transactions on*, vol. 13, no. 6, pp. 739–750, 2004.

[25] W. W. Boles and B. Boashash, "A human identification technique using images of the iris and wavelet transform," *IEEE Transactions on Signal Processing*, pp. 1185–1188, 1998.

[26] T. S. Lee, "Image representation using 2d gabor wavelets," *IEEE transactions on pattern analysis and machine intelligence*, vol. 18, October 1996.

[27] L. Masek, "Recognition of human iris patterns for biometric identification," 2003.

[28] D. Carr, "Iris recognition: Gabor filtering." `http://cnx.org/content/m12493/latest/`, December 2004. Datum bezocht: 10 augustus 2011.

[29] H. Cruse, "Neural networks as cybernetic systems." `http://www.brains-minds-media.org/archive/290`. Datum bezocht: 10 augustus 2011.

[30] Chinese Academy of Sciences, "Casia iris image database," November 2013. http://http://www.idealtest.org/.